

## Production of highly charged slow Ar ions recoiled in 1.05-MeV/amu $\text{Ne}^{q+}$ ( $q=2,7-10$ ) and $\text{Ar}^{q+}$ ( $q=4,6,10-14$ ) -ion bombardment

T. Tonuma, H. Shibata,\* S. H. Be, H. Kumagai, M. Kase, T. Kambara, and I. Kohno  
*Institute of Physical and Chemical Research, 2-1 Hirosawa, Wakoshi, Saitama 351, Japan*

A. Ohsaki  
*Institute for Molecular Science, Okazaki-shi, Aichi 444, Japan*

H. Tawara  
*Institute of Plasma Physics, Nagoya University, Chigusa-ku, Nagoya 464, Japan*  
 (Received 30 September 1985)

The partial cross sections for production of slow recoil  $\text{Ar}^{i+}$  ions in 1.05-MeV/amu  $\text{Ne}^{q+}$  ( $q=2,7-10$ ) and  $\text{Ar}^{q+}$  ( $q=4,6,10-14$ ) -ion impact have been determined. It is confirmed that the partial cross sections are dependent upon the charge state  $q$  of  $\text{Ne}^{q+}$  and  $\text{Ar}^{q+}$  ions but not significantly on the projectiles themselves. The measured partial cross sections were compared with the independent-electron approximation for low-charge-state recoil ions which were produced in collision with large impact parameters and with the "compound atom" model for high-charge state of the recoil ions which were produced in relatively close collisions. Experimental data were appreciably well reproduced by the combination of the approximation and the model.

### I. INTRODUCTION

It is well established from Auger and x-ray spectral features that fast, heavy-ion bombardment can produce multiple ionization of atoms in a single collision.<sup>1</sup> As a result, slow highly charged target recoil ions are produced. These low-velocity highly charged recoil ions have recently been used as an ion source to study the electron-capture process at low energies.<sup>2,3</sup>

Cocke<sup>4</sup> has systematically measured the cross sections for production of recoil ions under single collisions between 25 and 45 MeV Cl ions and targets of He, Ne, and Ar as a function of the incident projectile ion charge state. Recently, Ullrich *et al.*<sup>5</sup> and Kelbch *et al.*<sup>6</sup> have measured slow recoil ion production cross sections in highly charged ion impact which were found to be quite large, e.g.,  $3.5 \times 10^{-18}$  cm<sup>2</sup> for production of  $\text{Ar}^{18+}$  ions in 15.5-MeV/amu  $\text{U}^{75+}$ -ion impact. Gray *et al.*<sup>7</sup> have measured cross sections for production of highly charged low-velocity recoil Ne ions by 1-MeV/amu C, N, O, and F projectiles by identifying the final-charge states of both the low-velocity recoil ion and high-velocity projectile ion through coincidence technique. Their result shows that, for a given incident-projectile charge state, the charge-state distribution of the recoil ions is strongly correlated to the final charge state of the projectiles. The single- and double-electron-capture events by the incident ions during collision have been found to cause significant shifts in the recoil ion charge-state distribution toward higher charge state. In a similar experiment Kelbch *et al.*<sup>8</sup> have recently measured the recoil ion production cross sections in collisions of 2 MeV/amu  $\text{Br}^{q+}$  ( $q=14-27$ ) ions with Ne target atoms and found that the direct multiple ionization is the dominant process for the production of low-charge-state recoil ions whereas the production of highly

charged recoil ions is accompanied by the electron capture into projectile ions from target Ne K shell. They explained successfully the experimental data with the independent electron approximation (IEA) summarized by McGuire and Weaver.<sup>9</sup> However, up to now, there are no theories which can well reproduce the experimental results on the production of highly charged recoil ions in ion impact over a wide range of the recoil ion charge and over a wide range of the collision energies.

In this paper we report experimental results of the partial ionization cross sections of slow recoil ions produced in collisions of 1.05-MeV/amu  $\text{Ne}^{q+}$  ( $q=2,7-10$ ) and  $\text{Ar}^{q+}$  ( $q=4,6,10-14$ ) ions with Ar target atoms and compare them with the calculation of Olson<sup>10</sup> by the classical trajectory Monte Carlo method (CTMC). Also, the observed cross sections are compared with the IEA applied for production of low-charge-state  $\text{Ar}^{i+}$  recoil ions in collisions with large impact parameters. Those for higher-charge-state  $\text{Ar}^{i+}$  recoil ions are compared with the "compound atom" model<sup>11</sup> which determines the charge-state distribution of recoil ions produced in close collisions.

### II. EXPERIMENTAL PROCEDURE

The present measurements of the charge-state distribution of slow recoil Ar ions were made using the apparatus shown in Fig. 1. A beam of  $\text{Ne}^{q+}$  ( $q=2$ ) and  $\text{Ar}^{q+}$  ( $q=4,6$ ) ions from the heavy-ion linear accelerator of the Institute of Physical and Chemical Research intersected at right angles a stream of Ar gas emerging from a single tube nozzle. The charge state  $q$  of the incident  $\text{Ne}^{q+}$  ( $q=7-10$ ) and  $\text{Ar}^{q+}$  ( $q=10-14$ ) ions was selected by a switching magnet after passing through a carbon foil, the ion intensity with  $q=8$  for Ne and  $q=12$  for Ar ion be-

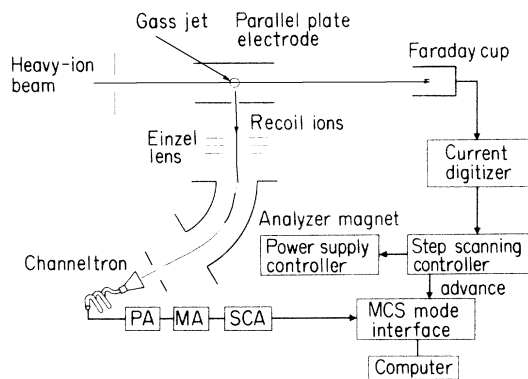


FIG. 1. Schematic diagram of the apparatus.

ing maximum at the present projectile energy. The beam spot was defined with two slits about 1 m upstream from the target, and was about 0.7 mm wide and 2 mm high on the target. Low-velocity recoil ions produced in the collision were extracted by an electric field applied perpendicularly to the primary beam direction, analyzed by a double focusing magnet with the orbit radius of 15 cm and the deflection angle of  $60^\circ$ , and finally detected by a channeltron at the focusing point of the magnet. The charge-state spectra of the recoil ions were obtained by

scanning the magnetic field and counting the detected ions with a multichannel scalar. A typical charge-state spectrum of slow recoil Ar ions produced by 1.05-MeV/amu  $\text{Ne}^{9+}$  beam bombardment on the Ar target is shown in Fig. 2. Ar ions with the charge state from  $1+$  to  $12+$  were observed, together with traces of  $\text{H}^+$ ,  $\text{H}_2^+$ ,  $\text{O}^+$ ,  $\text{OH}^+$ ,  $\text{H}_2\text{O}^+$ ,  $\text{N}_2^+$ , and  $\text{O}_2^+$  as background peaks.  $^{36}\text{Ar}^+$  ions were also clearly observed and their ratio to  $^{40}\text{Ar}^+$  ions was in agreement with the natural abundance of 0.34% for Ar.

In the present measurement the slow recoil ions ( $\text{Ar}^{i+}$ ) were extracted at 1.5 kV and the bias of  $-3$  kV was applied on the front face of the channeltron. Therefore, the recoil ion energy arriving at the channeltron is  $4.5 \times i$  keV. The data<sup>12</sup> show that the relative detection efficiency for  $\text{Ar}^+$  ions above 3 keV is constant with uncertainties of about 10%. Fricke *et al.*<sup>13</sup> also reported that no change of the measured detection efficiency on the ion energy in the range from 4 to 15 keV and on the charge state up to  $6+$  was observed. Thus, the detection efficiency of the channeltron used for ions of different energy and charge state in the present experiment was assumed to be constant. As no ion sources capable of providing such highly charged ions are easily available, no direct experimental determination of the absolute transmission efficiencies through an acceleration-analyzing system is usually possible. However, in the present type of experiment, the abso-

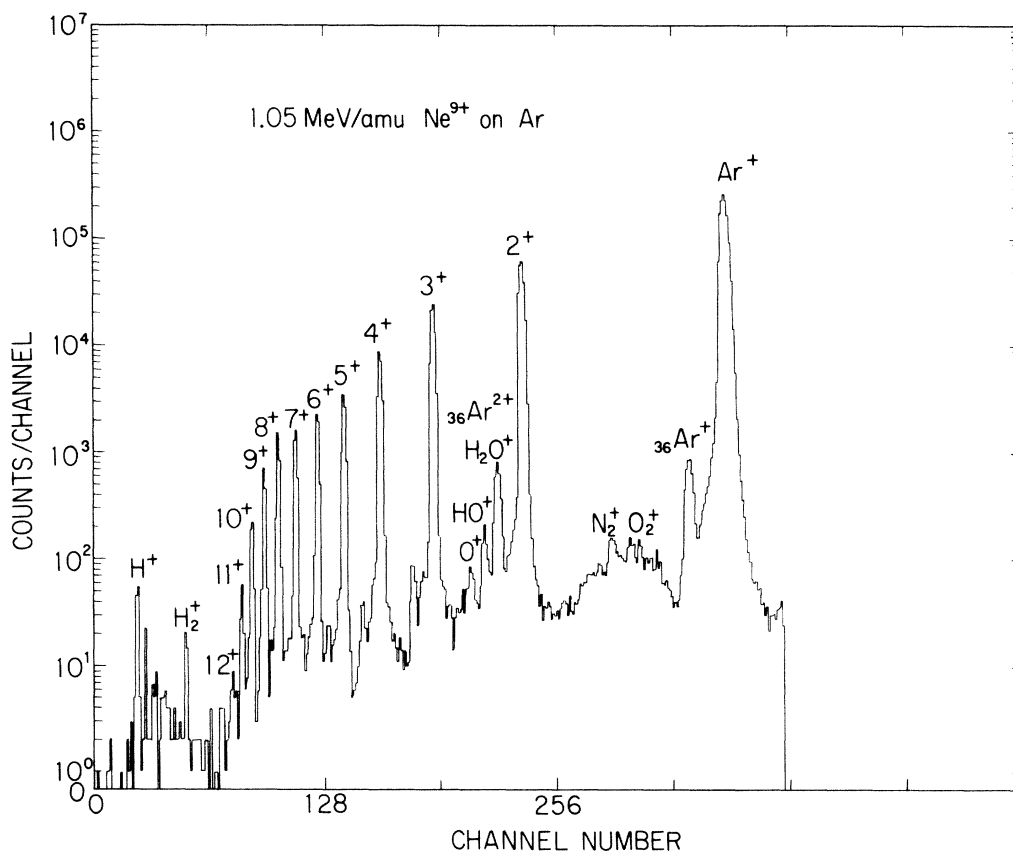


FIG. 2. Typical charge-state spectrum of recoil Ar ions produced by 1.05-MeV/amu  $\text{Ne}^{9+}$ -ion bombardment of Ar target. The beam current was about 3 nA. The channel was advanced in proportion to the magnetic field with 20 nC of the integrated beam charge on the Faraday cup.

lute efficiencies are not always necessary to know but it is good to know the relative transmission efficiencies which in the present work have been investigated through analysis of the ion orbits and experimentally optimizing the ion optic system. Then, the relative transmission efficiencies of ions with various charges are assumed to be constant. Recoil ions produced were measured as a function of the target Ar gas pressure. The yields of the recoil Ar ions in each charge state were found to increase linearly with the gas pressure up to  $3 \times 10^{-6}$  Torr from a typical background pressure of  $8 \times 10^{-8}$  Torr, measured at the chamber wall. This ensured that the observed recoil ions were produced under single-collision conditions. The mass spectroscopy method has an advantage of observing carefully a limited region of the high-charge-state spectrum of recoil ions, of which the counting rate is too low, without any disturbance of the gain loss of the channeltron due to high counting rate of low-charge-state recoil ions. Taking into account uncertainties in the detection efficiency, background subtraction, and collection efficiency, we place an error of 15% for the relative yields obtained in low-charge ions. However, the yields of high-charge recoil ions were small and, therefore, their statistical uncertainties increased with increasing charge and were about 50% for the highest-charge recoil ions. Combining absolute total net ionization cross sections,<sup>14</sup> which are determined through the parallel-plate method using standard technique (see the detailed description in Ref. 14), with the relative yields of recoil ions, absolute partial cross sections for production of recoil  $\text{Ar}^{i+}$  ions in collisions of 1.05 MeV/amu  $\text{Ne}^{q+}$  and  $\text{Ar}^{q+}$  ions with Ar targets were determined, as shown in Fig. 3.

### III. RESULTS AND DISCUSSION

#### A. Comparison with CTMC and IEA in recoil Ar ions with low charge

As shown in Fig. 3, the partial ionization cross sections are varied smoothly as a function of the projectile charge state  $q$  of  $\text{Ne}^{q+}$  and  $\text{Ar}^{q+}$  ions and appear to be almost independent of the projectiles. Eight  $M$ -shell electrons in Ar target are ionized dominantly in distinct collisions. Olson<sup>10</sup> calculated the cross section  $\sigma_i$  for ejecting  $i$  electrons in the  $M$  shell based upon the CTMC method. The dotted lines in Fig. 3 are the results of his calculation for the projectile energy of 1 MeV/amu. The present measurements of total net ionization cross sections ( $\sum_i i \sigma_i$ ) and total cross sections ( $\sum_i \sigma_i$ ) agree with the CTMC calculations within a factor of 2 for a wide range of the projectile charge state though the dependence on projectile charge  $q$  is slightly different. However, the theoretical partial ionization cross section  $\sigma_i$  is underestimated for small  $i$  and overestimated for large  $i$ , as already noted by Schlachter *et al.*<sup>15</sup> In the CTMC method, it is assumed that the projectile is fully stripped, whereas in most experiments, partially stripped ions are used. Thus, the calculated cross sections for production of low-charge state of the recoil ions for a given projectile charge state are underestimated possibly due to (i) the neglect of interactions of projectile electrons with target electrons, and (ii) the

fact that the target electrons will see a higher effective charge for small impact-parameter collisions. If the collision is not sufficiently sudden, electrons are ionized sequentially and the last few electrons to be ionized from a particular shell have the binding energies much larger than the average value. Then this approximation is not valid any more. Thus the calculations will generally overestimate the cross sections for the production of higher-charge-state ions. The Auger processes, which follow the innershell ionization due to the quasimolecular formation and electron-capture processes, also contribute significantly to the production of highly charged recoil ions. The contributions from these mechanisms are not included in this calculation.

For further analysis of the low-charge-state recoil  $\text{Ar}^{i+}$  ions we applied the IEA (Ref. 9) which assumes binomial statistics to be valid for multiple ionization. The partial cross section  $\sigma_i$  for ionizing  $i$  electrons can be obtained by integrating over the impact parameters  $b$ :

$$\sigma_i = 2\pi \int_0^\infty P_M^{(i)}(b) b db, \quad (1)$$

where  $P_M^{(i)}$  is the probability for ionizing  $i$  electrons in  $M$

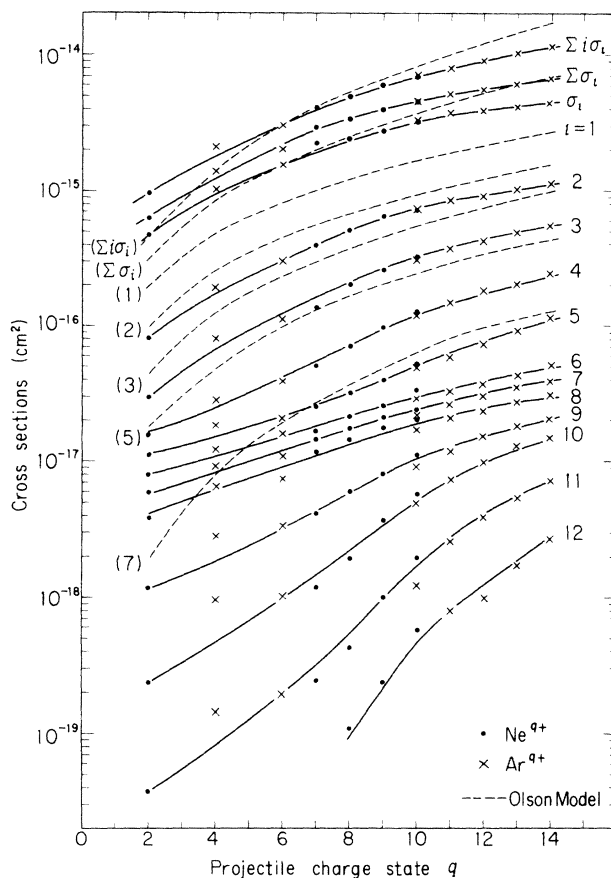


FIG. 3. Total net cross section  $\sum_i i \sigma_i$ , total cross section  $\sum_i \sigma_i$ , and partial cross section  $\sigma_i$  for production of the recoil  $\text{Ar}^{i+}$  ions as a function of the projectile charge  $q$  of 1.05 MeV/amu  $\text{Ne}^{q+}$  ( $\bullet$ ) and  $\text{Ar}^{q+}$  ( $\times$ ). The dotted lines represent the CTMC calculation of Olson for the projectile energy of 1 MeV/amu. The solid lines are drawn to guide eyes through experimental data.

shell and is defined by

$$P_M^{(i)}(b) = \binom{8}{i} P_M^i(b) [1 - P_M(b)]^{8-i}, \quad (2)$$

where  $\binom{8}{i}$  is the binomial coefficient.  $P_M(b)$  is the ionization probability of a single  $M$ -shell electron at the impact parameter  $b$  and can be empirically determined from the experimental data by assuming the following form:

$$P_M(b) = P_M(0) \exp(-b/r_M), \quad (3)$$

which has been proved to be adequate for large impact parameters.<sup>16</sup>  $P_M(0)$  and  $r_M$  can be determined by fitting Eq. (1) to the experimental data. The results for  $\text{Ne}^{2+}$  and  $\text{Ne}^{8+}$  ion impact are shown in Fig. 4(a). Similar results for  $\text{Ar}^{4+}$  and  $\text{Ar}^{14+}$  ion impact are shown in Fig. 4(b). This simple model gives a good description of the experimental data  $\sigma_i$  up to the recoil ion charge state  $i=3-4$  in  $\text{Ne}^{q+}$  ion and  $i=4-6$  in  $\text{Ar}^{q+}$ -ion impact. Figure 4(c) shows the results in  $\text{Ne}^{10+}$  and  $\text{Ar}^{10+}$ -ion impact. Experimental data up to the recoil-ion charge state  $i=5$  are well reproduced by the calculation with practically the same parameters for both  $\text{Ne}^{10+}$  and  $\text{Ar}^{10+}$ -ion impact. It is noted that the partial cross sections for both projectiles with the same charge  $q=10$  are practically the same. The values of  $P_M(0)$  and  $r_M$  determined by fitting the experimental data are plotted as a function of the projectile charge state  $q$  of  $\text{Ne}^{q+}$  and  $\text{Ar}^{q+}$  ions as shown in Fig. 5. The values of  $P_M(0)$  increase slightly with increasing the projectile charge state  $q$ . This indicates that the charge-state distributions of recoil ions are varied slowly with the projectile charge state. The values of  $r_M$

determining the absolute cross sections of production for recoil ions increase with increasing the projectile charge state  $q$ . It is also found from the figure that  $P_M(0)$  and  $r_M$  depend on only the charge state  $q$  of projectile ions and are almost independent of the projectiles themselves. This is the same conclusion as is in the calculation by Olson.<sup>10</sup>

However, the deviation of the experimental data from the calculation for higher charge state  $i$  becomes significant with increasing the charge state of recoil ions, and the experimental values are much larger than the calculation, indicating that the recoil Ar ions in higher charge state are produced not only by direct ionization, but also by other processes such as charge-transfer ionization and Auger processes.

### B. Data analysis of recoil Ar ions in high-charge states by the compound-atom model

Recently Meron and Rosner<sup>11</sup> have developed the compound-atom model based on the assumption of randomization of the electrons' motion during collisions and have reproduced well the observed charge-state distribution of the projectile ions in small-impact parameter collisions. We applied this model for analysis of high-charge-state recoil Ar ions observed in the present work. The main assumption of the model is that during a close collision some electrons of both projectile and target atoms, which are not altogether thrown out of the system, create a common structureless electron cloud which is later redistributed between both atoms. In the model the

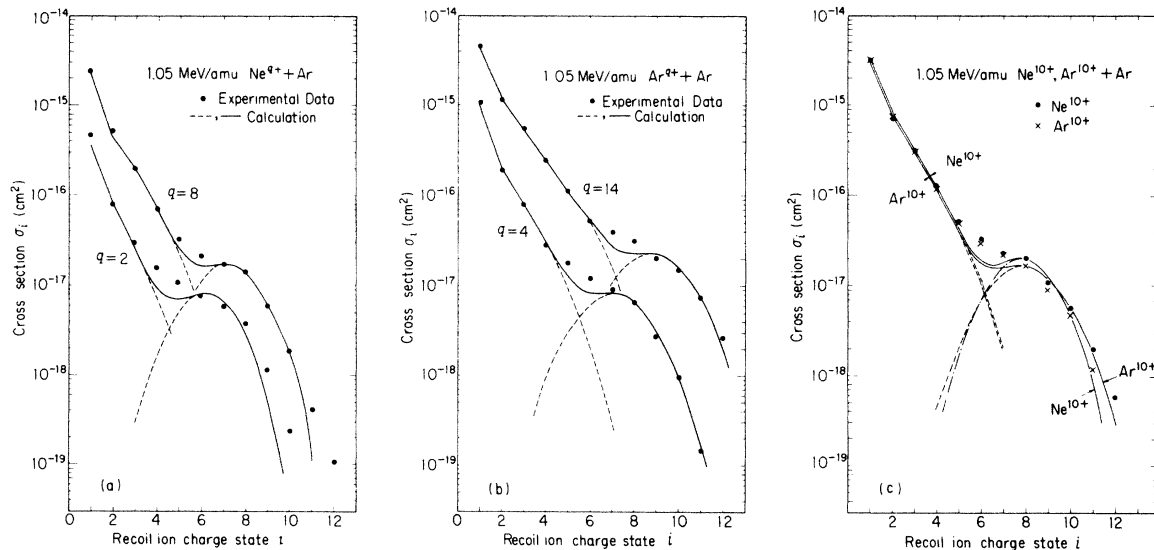


FIG. 4. (a) Partial ionization cross sections of recoil Ar ions in collisions of 1.05-MeV/amu  $\text{Ne}^{q+}$  ( $q=2$  and  $8$ ) ions with Ar atoms as a function of the recoil-ion charge state  $i$ . Solid points are the experimental data. The dashed lines on the left-hand side are the calculation determined by the IEA. The dotted lines on the right-hand side are the charge-state distribution calculated by the compound-atom model where the peak values of the distribution were adjusted by the experimental data. The solid lines represent the sum of calculations by the IEA and by the compound-atom model. (b) Partial ionization cross sections of recoil Ar ions in 1.05-MeV/amu  $\text{Ar}^{q+}$  ( $q=4$  and  $14$ ) ions on Ar atoms against the recoil-ion charge state  $i$ . Other explanations are the same as in (a). (c) Partial ionization cross sections of recoil Ar ion in 1.05-MeV/amu  $\text{Ne}^{10+}$  and  $\text{Ar}^{10+}$  ions on Ar atoms against the recoil-ion charge state  $i$ . Other explanations are the same as in (a).

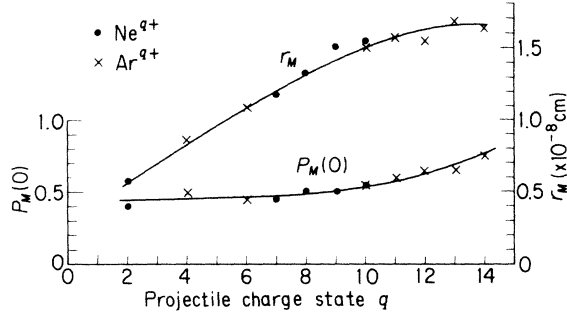


FIG. 5.  $P_M(0)$  and  $r_M$  obtained by fitting to the experimental data as a function of the projectile charge state  $q$ .  $P_M(0)$  and  $r_M$  are defined by Eq. (3). Solid lines are drawn to guide the eye.

compound atom is initially composed of  $N_i$  electrons in the common cloud and at the final stage  $N_f$  electrons remain in the cloud after some electrons are ejected. That is,  $N_i - N_f$  electrons are ejected before a quasistable common cloud is created. We assume that no further ionization of electrons occurs before separation once the quasistable common electron cloud is formed.<sup>17</sup> Then,  $N_f$  electrons are divided into  $N_1$  and  $N_2$  electrons which are the average numbers of electrons and recaptured into the projectiles with the nuclear charge  $Z_1$  and the recoil ions with  $Z_2$ , respectively, namely

$$N_f = N_1 + N_2 . \quad (4)$$

According to this model, the probability  $P_i^{N_f}$  that out of  $N_f$  electrons  $i$  electrons escape from the recoil atom is given by

$$P_i^{N_f} = \frac{\left[ \begin{array}{c} N_f \\ Z_2(u_c) - i \end{array} \right] \left[ \begin{array}{c} Z_1(u_c) + Z_2(u_c) - N_f \\ i \end{array} \right]}{\left[ \begin{array}{c} Z_1(u_c) + Z_2(u_c) \\ Z_2(u_c) \end{array} \right]} , \quad (5)$$

where  $Z_1(u_c)$  and  $Z_2(u_c)$  are the effective numbers of electrons in the projectile and the target atoms, respectively, involved in forming a common electron cloud whose velocity is smaller than a critical velocity  $u_c$ . (Electrons with velocities larger than  $u_c$  behave like spectators. For the detailed definition and the notation, see the original text.) In other words,  $P_i^{N_f}$  represents the probability of having the recoil ions with the charge state  $i$ .

The calculated parameters in this model in collisions of 1.05 MeV/amu  $\text{Ne}^{q+}$  and  $\text{Ar}^{q+}$  ions with Ar targets are given in Table I. The initial number of electrons  $N_i$  in the common cloud is given by

$$N_i = Z_1(u_c) + Z_2(u_c) - q , \quad (6)$$

where  $q$  is the projectile charge state and the mean charge  $\langle i \rangle$  of the recoil ions is given by  $\langle i \rangle = Z_2(u_c) - N_2$ . The fact that  $Z_2(u_c) = 16.35$  in the present case means that two electrons in the  $K$  shell of Ar atoms do not contribute significantly to forming the common electron cloud in the compound atom. In the process from the initial number of electrons  $N_i$  to the final number of electrons  $N_f$  in the common cloud, the  $(N_f - N_i)$  electrons are ejected, as mentioned already. The number of electrons ejected in this process decreases with increasing the projectile charge state  $q$  as indicated in Table I. The mean charge  $\langle i \rangle$  of recoil Ar ions clearly increases with increasing the projectile charge  $q$ . However, the dependence of  $\langle i \rangle$  on the projectile charge state  $q$  is slightly different between  $\text{Ne}^{q+}$

TABLE I. Parameters calculated by the compound-atom model in collisions of 1.05-MeV/amu  $\text{Ne}^{q+}$  and  $\text{Ar}^{q+}$  -ion impact with Ar target.  $N_i$  and  $N_f$  are the initial and final numbers of electrons in the common electron cloud.  $N_1$  and  $N_2$  are the average numbers of electrons redistributed into the projectile and the recoil ion from  $N_f$ .  $\langle i \rangle$  is the mean charge of the recoil ions given by  $\langle i \rangle = Z_2(u_c) - N_2$ .  $Z_1(u_c)$  and  $Z_2(u_c)$  are the effective numbers of electrons in the projectile and the target atom contributing to forming a common electron cloud. The detailed description of the parameters can be found in the text (Ref. 11).

	$q$	$N_i$	$N_f$	$N_1$	$N_2$	$\langle i \rangle$
<b>Ne<sup>q+</sup>-ion impact</b>						
$Z_1(u_c) = 9.55$	2	23.9	16.7	6.2	10.5	5.9
$Z_2(u_c) = 16.35$	7	18.9	15.0	5.5	9.5	6.9
	8	17.9	14.5	5.3	9.2	7.2
	9	16.9	14.0	5.2	8.8	7.6
	10	15.9	13.5	5.0	8.5	7.9
<b>Ar<sup>q+</sup>-ion impact</b>						
$Z_1(u_c) = Z_2(u_c)$	4	28.7	18.6	9.3	9.3	7.1
$= 16.35$	6	26.7	18.1	9.1	9.1	7.3
	10	22.7	16.8	8.4	8.4	8.0
	11	21.7	16.5	8.3	8.3	8.1
	12	20.7	16.1	8.1	8.1	8.3
	13	19.7	15.6	7.8	7.8	8.6
	14	18.7	15.1	7.6	7.6	8.8

and  $\text{Ar}^{q+}$ -ion impact.

The charge-state distributions of recoil Ar ions determined by Eq. (5) are shown in Figs. 4(a)–4(c). The peak values of the distribution, the only single free parameter in this model, were adjusted to fit the experimental data. The solid lines in these figures represent the sum of both IEA and compound-atom-model calculations. As seen from Figs. 4(a)–4(c), the distributions are very similar to Gaussian distributions and the mean charges of the distribution increase with increasing the projectile charge state  $q$ . The calculated charge-state distributions for  $\text{Ar}^{q+}$ -ion impact reproduce the experimental data somewhat better than those for  $\text{Ne}^{q+}$ -ion impact. In fact, the deviation in  $\text{Ne}^{q+}$ -ion impact is clearly observed at higher charge states, suggesting that this model is more effective for relatively symmetric collision systems having similar numbers of electrons in both projectile and target atoms. Comparing the charge-state distributions for  $\text{Ne}^{10+}$ -ion impact with those for  $\text{Ar}^{10+}$ -ion impact with the same projectile charge state as shown in Fig. 4(c), it is found that the width of the distribution for  $\text{Ne}^{10+}$  is slightly narrower than that for  $\text{Ar}^{10+}$ -ion impact, though the mean charges of the distribution are almost the same for both ion impact. It is also noted that the calculated mean charge for the lower projectile charge state is found to be different between  $\text{Ne}^{q+}$  and  $\text{Ar}^{q+}$ -ion impact and the difference increases with decreasing the projectile charge state (see Table I) and also the widths of the distribution tend to be narrow for the low atomic number of the projectiles. Therefore, it is concluded that although the charge-state distribution of the recoil ions estimated by the compound-atom model tends to be underestimated for low- $Z$  projectiles, this model can generally reproduce the experimental data on the charge distribution at higher charge.

### C. Comparison of the present partial cross sections of Ar ions with those in other projectiles

Figure 6 shows a comparison of the present results of the partial ionization cross sections of Ar ions produced in 1.05 MeV/amu  $\text{Ne}^{2+}$  and  $\text{Ar}^{14+}$ -ion impact with those in protons by Wexler<sup>18</sup> and DuBois *et al.*<sup>19</sup> and in electron impact by Schram,<sup>20</sup> the projectile velocities being nearly equal. As seen in Fig. 6, the present data show some structure due to the electronic shells of Ar targets which can be reproduced fairly well with the compound-atom model as described in the previous section; relatively large cross sections for production of  $\text{Ar}^{i+}$  ( $i \geq 7$ ) ions corresponding to the ionization of the  $3s$  shell electrons, compared with that for  $\text{Ar}^{6+}$  ions, should be due to the contribution of the  $2p$  inner-shell ionization. The results in  $\text{Cl}^q$  ion impact by Cocke,<sup>4</sup> not included in Fig. 6 to avoid the complication, are very similar to the present results, though his absolute values are somewhat larger than ours. As can be seen, the cross sections for production of singly charged  $\text{Ar}^{1+}$  ions are nearly equal in both 570-eV-electron and 1-MeV-proton impact, showing that  $\text{Ar}^+$  ions are dominantly produced by the direct ionization process. Obviously the partial cross sections of higher charged ions are much higher (almost 1 order of magni-

tude for  $i=4-5$ ) for 1-MeV protons than for 570-eV electrons. This indicates the contribution from other processes, namely, the electron capture by protons from the target in proton impact. In fact, the cross sections of  $L$ -shell electron capture from Ar atoms into protons were measured to be about  $7 \times 10^{-20} \text{ cm}^2$  at the present collision energy<sup>21</sup> which is comparable to those of production of recoil  $\text{Ar}^{4+}$  and  $\text{Ar}^{5+}$  ions. This figure demonstrates clearly that the production cross sections of highly charged recoil ions are much higher for highly charged heavy-ion impact than for protons and electrons, and the difference among them increases progressively with increasing the recoil ion charge. Also shown, for a further comparison, are the partial cross sections of  $\text{Ar}^{i+}$ -ion production in 15.5-MeV/amu  $\text{U}^{75+}$ -ion impact<sup>6</sup> which is the highest projectile charge ever used in recoil ion production.

## IV. CONCLUSIONS

The partial cross sections for production of highly charged recoil  $\text{Ar}^{i+}$  ions in 1.05-MeV/amu  $\text{Ne}^{q+}$  ( $q=2,7-10$ ) and  $\text{Ar}^{q+}$  ( $q=4,6,10-14$ )-ion impact have been determined by measuring total net ionization cross sections and fractions of the recoil ions. The measured partial cross sections of recoil Ar ions in low charge states were compared with the independent electron approximation and it is found that  $P_M(0)$  and  $r_M$ , defined by Eq. (3)

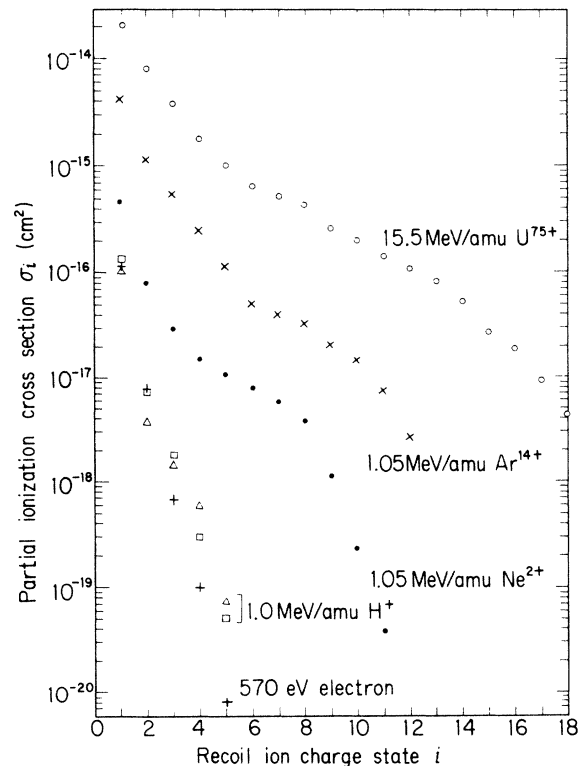


FIG. 6. Partial ionization cross sections of recoil  $\text{Ar}^{i+}$  ions in various projectile impact on Ar atoms. +: 570-eV electrons, Schram (Ref. 20);  $\square$ : 1-MeV proton, Wexler (Ref. 18);  $\triangle$ : 1-MeV proton, DuBois *et al.* (Ref. 19);  $\bullet$ : 1.05-MeV/amu  $\text{Ne}^{2+}$ . Present results:  $\times$ , 1.05-MeV/amu  $\text{Ar}^{14+}$ ;  $\circ$ : 15.5-MeV/amu  $\text{U}^{75+}$ , Kelbch *et al.* (Ref. 6).

and determined by fitting to the experimental data, depend on only the projectile charge state  $q$  of  $\text{Ne}^{q+}$  and  $\text{Ar}^{q+}$  and are independent of the projectile themselves. The partial cross sections of recoil Ar ions in high charge states were compared with the compound-atom model which determine the charge-state distribution and were appreciably well reproduced by this model in the present collision system. Therefore, it can be concluded that the combination of the independent-electron model based on the direct ionization and the compound-atom model based on the formation of the common cloud during collision reproduce well the experimental data on the charge distri-

bution of recoil  $\text{Ar}^{i+}$  ions produced in 1.05-MeV/amu  $\text{Ne}^{q+}$  and  $\text{Ar}^{q+}$ -ion impact over a wide range of the charge state  $i$ .

#### ACKNOWLEDGMENTS

One of the authors (T.T.) would like to thank Dr. A. Yagishita for help in designing the apparatus and Dr. T. Watanabe and Dr. Y. Awaya for their support of the present work. Also, one of the authors (H.T.) would like to acknowledge the partial support of a grant-in-aid of the Ministry of Education, Science and Technology, Japan.

---

\*Present address: Research Center for Nuclear Science and Technology, University of Tokyo, 2-22 Shirakata-shirane, Tokai-mura, Ibaraki 319-11, Japan.

<sup>1</sup>N. Stolterfoht, *Fundamental Processes in Energetic Atomic Collisions* (Plenum, New York, 1983), p. 295.

<sup>2</sup>C. R. Vane, M. H. Prior, and R. Marrus, *Phys. Rev. Lett.* **46**, 107 (1981).

<sup>3</sup>C. Schmeissner, C. L. Cocke, R. Mann, and W. Meyerhof, *Phys. Rev. A* **30**, 1661 (1984).

<sup>4</sup>C. L. Cocke, *Phys. Rev. A* **20**, 749 (1979).

<sup>5</sup>J. Ullrich, C. L. Cocke, S. Kelbch, R. Mann, P. Richard, and H. Schmidt-Böcking, *J. Phys. B* **17**, L785 (1984).

<sup>6</sup>S. Kelbch, J. Ullrich, R. Mann, P. Richard, and H. Schmidt-Böcking, *J. Phys. B* **18**, 323 (1985).

<sup>7</sup>T. J. Gray, C. L. Cocke, and E. Justiniano, *Phys. Rev. A* **22**, 849 (1980).

<sup>8</sup>S. Kelbch, H. Schmidt-Böcking, J. Ullrich, R. Schuch, E. Justiniano, H. Ingwersen, and C. L. Cocke, *Z. Phys. A* **317**, 9 (1984).

<sup>9</sup>J. H. McGuire and L. Weaver, *Phys. Rev. A* **16**, 41 (1977).

<sup>10</sup>R. E. Olson, *J. Phys. B* **12**, 1843 (1979).

<sup>11</sup>M. Meron and B. Rosner, *Phys. Rev. A* **30**, 132 (1984).

<sup>12</sup>The Channeltron used is Model No. CEM 4039 manufactured by Galileo Electro-Optics Corp. The data are due to their "Data sheet 4000."

<sup>13</sup>J. Fricke, A. Müller, and E. Salzborn, *Nucl. Instrum. Methods* **175**, 379 (1980).

<sup>14</sup>S. H. Be, T. Tonuma, H. Kumagai, H. Shibata, M. Kase, T. Kambara, I. Kohno, and H. Tawara, Institute of Physical and Chemical Research (RIKEN) Accelerator Progress Report No. 18, 1984 (unpublished), p. 80; *J. Phys. B* (to be published).

<sup>15</sup>A. S. Schlachter, W. Groh, A. Müller, H. F. Beyer, R. Mann, and R. E. Olson, *Phys. Rev. A* **26**, 1373 (1982).

<sup>16</sup>P. H. Mokler and H. D. Lissen, *In Progress in Atomic Spectroscopy*, edited by H. F. Berger and H. Kleinpoppen (Plenum, New York, 1983), p. 321.

<sup>17</sup>We can expect an additional ejection of the outer electrons upon the separation of the target atom and the projectile ion, i.e.,  $N_f > N_1 + N_2$ . In order to estimate the additional ejection, Meron and Rosner introduced the cutoff parameters. However, these corrections become less meaningful as far as the upper cutoff velocity  $u_c$  is assumed to be  $2(v_1 + v_2)$  according to Eq. (5) in the text (Ref. 11) since the correction terms lose the velocity dependence in this situation.

<sup>18</sup>S. Wexler, *J. Chem. Phys.* **41**, 1714 (1964).

<sup>19</sup>R. D. DuBois, L. H. Toburen, and M. E. Rudd, *Phys. Rev. A* **29**, 70 (1984).

<sup>20</sup>B. L. Schram, *Physica (Utrecht)* **32**, 197 (1966).

<sup>21</sup>M. Rødbro, E. Horsdal Pedersen, C. L. Cocke, and J. R. Macdonald, *Phys. Rev. A* **19**, 1936 (1979).